Biochimica et Biophysica Acta, 679 (1982) 177–187
Elsevier Biomedical Press

BBA 41021

THE LOCATION OF REDOX CENTERS IN BIOLOGICAL MEMBRANES DETERMINED BY RESONANCE X-RAY DIFFRACTION

I. OBSERVATION OF THE RESONANCE EFFECT

J. STAMATOFF [a], P. EISENBERGER [a], J.K. BLASIE [b,c], J.M. PACHENCE [b,c], A. TAVORMINA [b,c], M. ERECINSKA [b], P.L. DUTTON [b] and G. BROWN [d]

[a] *Bell Laboratories, Murray Hill, NJ 07974,* [b] *Department of Biochemistry and Biophysics,* [c] *Department of Chemistry, University of Pennsylvania, Philadelphia, PA 19104 and* [d] *Stanford Synchrotron Radiation Laboratory, Stanford, CA 94305 (U.S.A.)*

(Received June 22nd, 1981)

Key words: Redox center; Resonance X-ray diffraction; Synchrotron radiation; Membrane reconstitution

We have developed resonance X-ray diffraction methods to locate for the first time intrinsic metal atoms associated with redox centers within biological membrane systems. The study of membranes containing dilute concentrations of resonant scatterers has been made possible by the development of synchrotron radiation sources of X-rays. The technique permits altering the scattering power of a particular atom relative to others by varying the incident X-ray energy. Thus, this method may be used to locate a metal atom within a complex integral protein without chemical modification of the membrane. We present resonance diffraction data taken with synchroton radiation for two different membrane systems: cytochrome oxidase incorporated into lipid vesicles and a photosynthetic reaction center-cytochrome *c* complex also reincorporated into lipid vesicles.

Introduction

The illumination of structure-function relationships is the focus of a large segment of biophysical research. The success of protein crystallography has made a major contribution to this effort. Many biological systems, however, cannot be crystallized so that this approach is not feasible. Biological membranes generally are in this category. Only in a few special cases is the structure crystalline within the membrane plane. However, membranes can be stacked in regular arrays and diffraction investigations provide structural information about the membrane. In these membrane studies, the diffraction patterns are of low to moderate resolution so that identification of particular moieties, such as amino acids, is not possible. Therefore, atomic coordinates are not known for biological membranes.

Reconstitution of membranes from a small number of molecular components provides simplified structures to study. Thus, cytochrome oxidase or photosynthetic reaction centers, both electron-transport proteins, may be extracted from their native membranes, purified, and reincorporated at relatively high concentration into a simple well defined lipid bilayer. Diffraction investigation then provides information, at low to moderate resolution, about the distribution and structure of the protein in the membrane. Understanding the mechanism for electron transport in these proteins will require considerable additional information. One key element of structural information is the location of the redox centers in the membrane profile.

Many redox centers contain metal atoms. If these metals could be isomorphically replaced by atoms of substantially different scattering power, then mea-

surement of changes in diffracted lamellar intensities even at low to moderate resolution combined with prior knowledge of the number of metal atoms sites within the membrane profile would permit accurate location of these sites. The high resolution accuracy in the determination of metal atom locations with low resolution data is the direct result of prior knowledge of the number of metal sites. Diffraction techniques which utilize isomorphous replacement and the method of accurate determination of the location of particular sites using low resolution data have been demonstrated for membrane systems by both X-ray [1] and neutron diffraction studies [23]. Unfortunately, the replacement of intrinsic metal atoms within cytochrome oxidase or bacterial photosynthetic reaction centers substantially alters the functionality of the membrane so that there is no obvious basis for assuming structural isomorphism.

The X-ray scattering power of an atom may be significantly changed at X-ray energies near the atom's absorption edge. By recording diffraction patterns at various X-ray energies about a metal atom's absorption edge, it is possible to locate the metal atom within a complex structure by methods similar to isomorphous replacement. Obviously, the metal atom is not chemically altered so that the membrane's functionality remains unchanged and the assumption of isomorphism between data sets collected at different X-ray energies is strictly valid. This ideal solution to the problem is known as resonance (or anomalous) X-ray diffraction. Until recently, changing X-ray energies required altering target metals in conventional X-ray tubes. The specific X-ray energies available did not allow one to maximize the resonant change in scattering power of a particular metal atom. The development of synchrotron radiation as a practical research source of X-rays permits easy and continuous alteration of X-ray energies while maintaining high incident fluxes. These advantages of synchrotron radiation for resonance scattering studies have been previously demonstrated for both biological [4–7] and nonbiological problems [8].

This paper, and the following one [9] describe the first application of resonance X-ray scattering to the location of metal atoms associated with redox centers in biological membranes. The experiment was conducted at the Stanford Synchrotron Radiation Laboratory and, thus, avails itself of the significant advantages of synchrotron radiation. The concentration of intrinsic metal atoms in these membranes formed with cytochrome oxidase or the photosynthetic reaction center-cytochrome *c* complex is very small (about 1 atom in 10^4). Therefore, detection of the resonance scattering effect on diffracted intensities is technicaly very difficult. This paper describes the experimental methods and detection of the resonance effect. The second paper [9] describes the application of the method to a known membrane profile structure as a test of the technique's validity for membrane systems.

Theory

We consider an oriented multilayer formed from stacks of collapsed unilamellar membrane vesicles. The unit cell profile then contains a pair of opposed single membrane profiles. Let the X-axis be orthogonal to the membrane plane. The following relationships hold:

$$F(h/D) = \sum_i f_i \cos(2\pi X_i h/D) \tag{1}$$

$$I(h/D) = |F(h/D)|^2 \tag{2}$$

$$\rho(X) = \sum_h F(h/D) \cos(2\pi X h/D) \tag{3}$$

where F is the structure factor for the unit cell profile, I is the diffracted intensity along X^* parallel to X where $|X^*| = 2 \sin\theta/\lambda = h/D$, ρ is the unit cell profile, i.e., the unit cell electron density projected on the X-axis, D is the membrane pair periodicity along the X-axis, h indexes a particular X-ray reflection, f_i is the atomic scattering factor for the ith atom and X_i is the X coordinate of the ith atom.

Note that the symmetry condition $\rho(X) = \rho(-X)$ is implicit in the above equations and is justified, in the X-axis projection, by the formation of pairs of opposing membranes in the creation of a multilayer.

It is well known that near an absorption edge, the general form for the atomic scattering factor is given by:

$$f(S, E) = f_0(S) + f'(S, E) + if''(S, E) \tag{4}$$

where $S = 2 \sin\theta/\lambda$ and E is the incident X-ray energy.

Here f_0 is the atomic scattering factor far away from an absorption edge. At small scattering angles, f_0 approximately equals the atomic number which is a positive real constant and is independent of the incident X-ray energy. The f' term denotes the change in the real component of the scattering factor as a function of energy. It is reasonably well described by Hönl theory [10,11] on a broad (kilovolt) scale entered about an absorption edge. For K-shell absorption edges, f' is negative and its energy dependence follows a roughly symmetric curve having a minimum at the edge. Near the K absorption edge, damping terms dominate but recent studies show that f' is unexpectedly large. (ref. 12 and Bienenstock, A., personal communication). The f'' term denotes the absorptive component which is also energy dependent. It is simply related to the atomic absorption coefficient [10,11]. It is zero below the absorption edge and rapidly rises at the edge in an approximate step function manner. For iron atoms at the edge, $f_0 \cong 26$ electrons, $f' \cong -8$ electrons, and $f'' \cong +5$ electrons [5,12].

Near the absorption edge, the structure factor for the unit cell profile is therefore given by:

$$F(h/D) = F_0(h/D) + F'(h/D) + iF''(h/D) \tag{5}$$

where all terms follow the form of Eqn. 1 except that the sum for the second and third terms extends only over the resonant atoms. Therefore, the diffracted intensity is given by:

$$I(h/D) = F_0^2(h/D) + 2F_0(h/D)F'(h/D) + F'^2(h/D) + F''^2(h/D) \tag{6}$$

For our systems the relative number of resonant scattering atoms is very small and, therefore, the magnitude of the resonant effect would generally be a small fraction of the scattering amplitude. For example, in the cytochrome oxidase system, each cytochrome oxidase molecule with the surrounding lipid molecules has a molecular weight of approx. 200 000. Thus, there are greater than 10^5 electrons in one complex. Each cytochrome oxidase molecule contains two iron atoms so that the magnitude of the f' effect should be about 16 electrons. At zero scattering angle all electrons contribute coherently so that F_0 has a magnitude of approx. 10^5 electrons. Hence, F'/F_0 is about $2 \cdot 10^{-4}$. At other scattering angles the effect is enhanced for reasons described below. In addition, f' magnitudes are not well determined and may be substantially larger [11]. Nevertheless, F' remains small with respect to F_0. Therefore:

$$\begin{aligned} |F_0(h/D)| &\gg |F'(h/D)| \\ |F_0(h/D)| &\gg |F''(h/D)| \end{aligned} \tag{7}$$

Hence Eqn. 6 is well approximated by:

$$I(h/D) \approx F_0^2(h/D) + 2F_0(h/D)F'(h/D) \tag{8}$$

This shows that the intensity changes which we should observe as a function of X-ray energy must follow that of f' and that the changes are enhanced by the cross term.

A second effect which enhances the resonance scattering effect is membrane contrast. In diffraction experiments, $I(0)$ is not observed but contributes a constant to the Fourier synthesis of the unit cell electron-density profile. Relative integrated intensities for all other reflections depend solely on the shape of the electron-density profile about the average level determined by $I(0)$. Absolute integrated intensities for the other reflections change proportionately with the magnitude of deviation about this average level (i.e. the contrast). For planar multilayers, the integrated intensity of a given reflection is proportional to the number of multilayers. Therefore, by determining absolute scattered intensity, it is possible to compare the contrast of different membrane systems. Our results show that both reconstituted membrane structures are of relative low contrast. This is a direct consequence of the structure of the lipid bilayer and reincorporated protein. The effect of incorporating integral protein into a lipid bilayer is to add electrons to less electron-dense regions and to distribute the more dense regions over a larger region of the membrane profile. Such electron-density distributions affect the contrast and, therefore, in general the magnitude of scattered intensity, $|F_0(h/D)|^2$ for $h \neq 0$. However, the distribution does not alter the magnitude of $F'(h/D)$ which is determined solely by the atomic $f'(E)$ magnitude and the position of the resonant scattering atom within the profile. Thus, lowering the contrast in general enhances $|F'(h/D)|/|F_0(h/D)|$ for $h \neq 0$. As an extreme example, if the profile were flat

(i.e., no contrast), no diffracted intensity would be observed except that due to resonance scattering effects.

Experimental Methods

Reconstituted membrane samples of cytochrome oxidase and bacterial photosynthetic reaction centers complexed with cytochrome *c* were prepared by methods previously described (Refs. 13–15; Tavormina, A., Erecinska, M. and Blasie, J.K., unpublished data). Unilamellar vesicle preparations were ultracentrifuged onto aluminium foil and then transferrred to a planar glass support. The sedimented pellets were partially dehydrated in an N_2 environment with controlled high humidity at 5°C. The oriented multilayers were then transferred to a temperature-controlled sample chamber on a goniometer for diffraction studies.

For the reconstituted cytochrome oxidase membranes, the iron atoms in heme *a* and a_3 were investigated by recording lamellar diffraction about the iron absorption edge. For reconstituted membranes containing the photosynthetic reaction center-cytochrome *c* complex the heme of cytochrome *c* was investigated. As a test of the resonance scattering method (see the following paper [9]), the iron atom of cytochrome *c* was replaced by cobalt using methods previously described [15]. Therefore, resonance X-ray scattering studies for this membrane were conducted about the cobalt absorption edge. Absorption edge energies were directly determined by X-ray absorption spectroscopy of cytochrome oxidase and cobalt-substituted cytochrome *c* in the membrane multilayer.

X-ray experiments were performed at the Stanford Synchrotron Radiation Laboratory. X-rays from the storage ring were focussed using a bent cylindrical mirror and monochromatized using two flat germanium ⟨111⟩ crystals. The energy resolution was estimated to be about 2 eV. This is substantially better than the typical 5–8 eV energy resolution for the system due to the fact that only a small portion of the beam is used. Monochromatized X-rays were defined by a slit (0.75 × 4 mm). The incident beam intensity was monitored by measuring the scattering from a thin plastic film with a scintillation detector. A second slit (0.86 × 4.28 mm) after the monitor served as a guard slit. The two input slits were separated by 288 mm using an evacuated path with mylar windows. Samples were sealed in a refrigerated specimen holder (about 5°C) in an N_2 environment at controlled relative humidity. Diffraction scans were performed using a large Huber diffractometer with two fixed slits and a scintillation detector on the 2θ arm. The first slit on the 2θ arm was placed at 128 mm from the sample and measured 1.55 × 6.65 mm. The second slit on the 2θ arm was separated from the first by an evacuated path with mylar windows. It measured 0.5 × 4.0 mm and was at 505 mm from the sample. The angular resolution, $\Delta 2\theta$, was defined by this last slit to be about 1 mrad.

Diffraction scans were performed at several energies about the iron or cobalt absorption edges. The absolute absorption edge energies were determined directly using cytochrome oxidase, photosynthetic reaction center, or cobalt-substituted cytochrome *c* samples. For these measurements, absorption edges were recorded by the fluorescence method using an intrinsic germanium detector. Figs. 1a and 2a show diffraction scans obtained from reconstituted cytochrome oxidase and photosynthetic reaction center-cytochrome *c* membrane multilayers. Each point of the scan represents the ratio of counts scattered to that observed by the monitor. Changes in X-ray intensities due to the storage ring's natural electron current decay or to electron beam instabilities within the storage ring make this procedure absolutely necessary.

The large changes in the lamellar diffraction with energy shown in Fig. 1b for a reconstituted cytochrome oxidase multilayer are not due to resonance scattering effects. There are several factors which determine this gross energy dependence. Nonresonant scattering depends strongly on X-ray energy for both the incident beam monitor and specimen [11]. X-ray absorption in the multilayer contributes a strong energy dependence. In addition, the diffractometer's geometry (e.g., fixed slits) imparts an energy dependence. With the exception of X-ray absorption by resonant atoms, these factors produce only a monotonic variation in diffracted intensity with no features at a particular absorption edge. The detection of weak (about 1–5%) diffracted intensity changes due to resonant effects in the presence of these large monotonic nonresonant changes (of the order of 20%

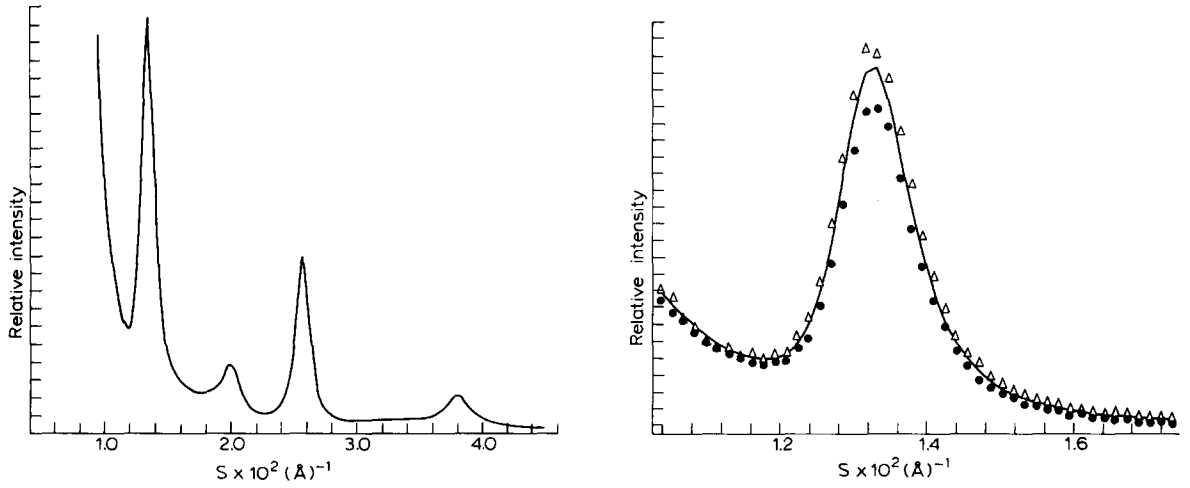

Fig. 1. (a) An averaged lamellar X-ray diffraction pattern from an oriented multilayer of reconstituted cytochrome oxidase membranes. Individual $\theta-2\theta$ scans, recorded with an incident X-ray energy at the iron K absorption edge, were averaged to produce this pattern. (b) Averaged lamellar X-ray diffraction at several X-ray energies for the second-order reflection ($h = 2$) from an oriented multilayer of reconstituted cytochrome oxidase membranes. (–) E = iron K absorption edge energy; (△) E = iron K absorption edge energy +200 eV; (■) E = iron K absorption edge energy –200 eV.

over 200 eV) is problematic. In addition, X-ray absorption by the resonant atoms will produce an abrupt feature at the absorption edge. We note that all of these energy-dependent factors have, at most, a very weak coupling with the scattering vector $S = 2\sin\theta/\lambda$ (i.e., momentum transfer) in the small angular region of our scans. Thus X-ray absorption, which is strongly dependent on energy, affects all diffractions peaks in approximately the same manner. Changes in the resolution of the diffraction scans at different energies,

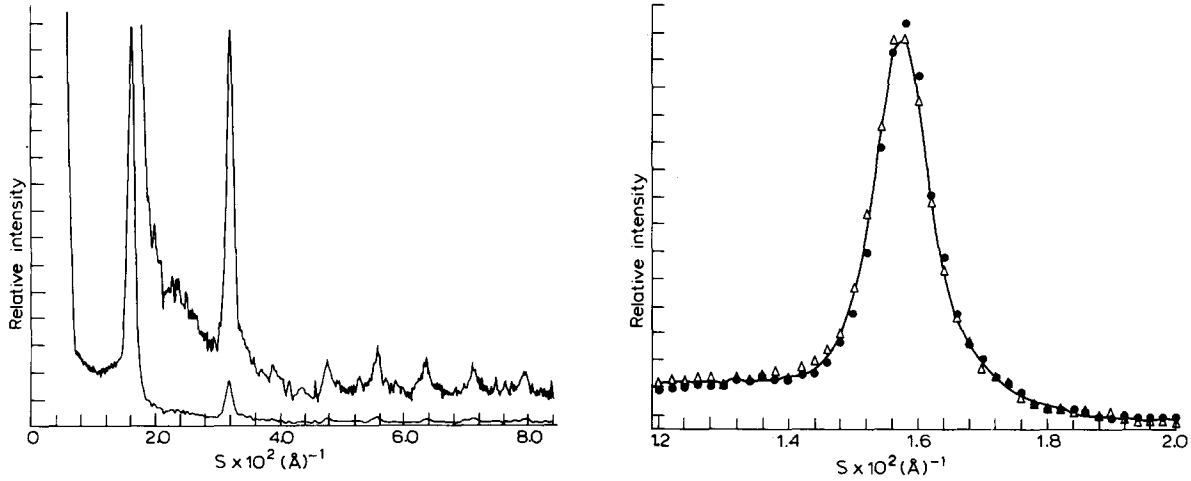

Fig. 2. (a) An average lamellar X-ray diffraction pattern from an oriented multilayer of reconstituted photosynthetic reaction center-cytochrome c membranes. Individual $\theta-2\theta$ scans recorded with an incident X-ray energy at the cobalt K absorption edge were averaged to produce this pattern. (b) Averaged lamellar X-ray diffraction at several X-ray energies for the second-order reflection ($h = 2$) from an oriented multilayer of reconstituted photosynthetic reaction center-cytochrome c membranes. (–) E = cobalt K absorption edge; (△) E = cobalt K absorption edge +200 eV; (■) E = cobalt K absorption edge –200 eV.

due to the use of a fixed slit, are the same for all diffraction peaks at a given energy. We therefore measure the energy dependence of the ratio of the integrated diffracted intensities of the lamellar reflections. Except for small and approximately linear deviations due to the absorption of nonresonant atoms, the utilization of the ratio of diffracted intensities eliminates the gross nonresonant energy dependencies. Furthermore, features due to absorption by resonant atoms are reduced to a magnitude far below the detection capability of this experiment.

In Fig. 2b, the intensity of the second diffraction order for a photosynthetic reaction center-cytochrome *c* multilayer is shown for X-ray energies about the cobalt absorption edge. Large changes of the diffracted intensity are not observed in comparison with the cytochrome oxidase multilayer (Fig. 1b). In this case, the sample is thinner, the incident X-ray energy is larger, and the sample mosaicity is smaller. As a result, the energy dependence happens to be more similar to that of the incident beam monitor. We have found that it is possible to minimize the gross energy-dependent variations in the integrated intensity by altering the thickness of the film used within the incident beam monitor. As a routine experimental procedure, altering the beam monitor was technically difficult and the use of ratios of integrated intensities proved to be a more suitable procedure.

Changes in ratios of diffracted intensities may occur from sample or storage ring instabilities. Small deviations of the sample's periodicity due to variations in water content can cause large changes in the ratio. For example, an about 30% change in the ratio of the second to fourth order integrated intensities corresponds to an approx. 1% change in the periodicity of a cytochrome oxidase membrane specimen. Movement of the electron beam in the storage ring can also subtly alter the angle of incidence on the sample or cause a small relative change between the incident beam monitor and specimen. To minimize both types of error, an averaging procedure was devised. A series of diffraction scans about the absorption edge performed such that linear changes in the ratio with time would not contribute to the energy dependence of the final averaged lamellar diffraction. For example, about the iron edge the series was 7125 eV, 7225 eV, 6925 eV, 7125 ... etc. Each scan took about 5 min. Series were completed within a fill of the storage ring. For a given series, scans at the same energy were then averaged to produce the final averaged lamellar diffraction at each energy which are centered about the same point in time.

As a final test to improve further the experimental accuracy, individual diffraction scans were examined for linear behavior. In this filtering procedure, the total integrated intensity (including background) for a given reflection and X-ray energy was plotted versus time. Series which contained intensities which varied nonlinearly in time (as judged by the least-square deviation from a line compared with the error expected based on counting statistics) were not used. Thus, we assure linearity so that the averaging procedure described above is valid.

Series which passes these tests were used to examine the energy dependence of the ratios of the integrated intensities. Scans at the same energy within a series were averaged to produce the final averaged lamellar diffraction at each energy. Peak-to-background ratios as well as peak and background shapes were substantially different for the two types of membrane samples. Therefore, slightly different analytical procedures were used for each. In general, background scattering was removed from each reflection for the final averaged lamellar diffraction at each energy. Errors in integrated intensities were found to be dominated by uncertainties in the background scattering rather than the stochastic error associated with the number of photons detected. Error bars for ratios of integrated intensities at each energy were therefore assigned based on the systematic variation of the points chosen as representative of background scattering about each lamellar reflection.

For reconstituted cytochrome oxidase multilayers, the following specific procedure was followed. Straight line backgrounds were fitted tangentially to plots of the logarithm of the averaged lamellar diffraction. Background regions were chosen on either side of a reflection such that the points within the selected region varied randomly about the tangential line. Straight line backgrounds were determined for all possible pairs of background points on either side of a reflection (i.e., if there are four possible points on the low-angle side of a peak and six background points on the high-angle side, 24 possible back-

grounds are determined). The straight lines were converted back to exponentially decaying curves and subtracted from the total lamellar diffraction.

Lamellar reflections were integrated after background removal over the region of the peak which exceeds 10 % of the peak height, thus excluding the wing regions from the integration. Peak areas were calculated for each of the possible pairs of background points and were then averaged to give the final area determination. The error (as percent error) caused by background removal was estimated from the standard deviation of the peak area values for each possible background. Ratios of the integrated lamellar reflections for different orders were calculated for each energy. Error bars (as percent error) for the ratios were determined to be the square root of the sum of the variances of the percent error for the contributing peak areas.

For reconstituted reaction center-cytochrome *c* membranes, the following specific procedure was used. The background scattering was determined by fitting a straight line through two points on either side of the logarithm of each lamellar reflection. As a first approximation, the points at $m = 1/2D, 3/2D, \ldots (2n+1)/2D$ were chosen as the background points (where D is the lattice periodicity and h/D the position of the center of lamellar reflection). The intensity of the background points was calculated as a five-point average about these $(2n+1)/2D$ locations. Next, a measure of peak symmetry was calculated for each reflection as the ratio of the integrated intensity on either side of the central value:

$$\int_{h/D-2\sigma}^{h/D} I(s, E)\,\mathrm{d}s \Big/ \int_{h/D}^{h/D+2\sigma} I(s, E)\,\mathrm{d}s \qquad (9)$$

The background points were systematically varied $(2n+1)/2D \approx \pm 5$ channels), and the peak symmetry values was calculated for each background pair in the same way. This was done for each lamellar reflection of every averaged lamellar diffraction pattern (it is possible that the background points can change with energy). The background pairs which produced peak symmetry values closest to unity, within the stochastic error of the integrated peak value, were chosen. In every case, more than one pair of background points gave analytically reasonable peak symmetry values.

Integration of reflections and their errors were determined in the same manner as for cytochrome oxidase samples. For these lamellar diffraction patterns, integrations were over the central region of the peak which exceeds 25% of the peak height.

Results

Fig. 3 shows the time variation of the integrated second-order reflection (including background) for a reconstituted cytochrome oxidase membrane multilayer. Each point represents the diffracted intensity relative to the incident beam monitor for a given diffraction scan taken at the iron K absorption edge. The line is determined by a least-squares fit through the points. Error bars are calculated for the stochastic error-based number of photons counted (including the error for the monitor). Similar plots were made for other energies in the series.

Fig. 4a shows the energy dependence of the ratios of the averaged integrated lamellar reflections for a reconstituted cytochrome oxidase membrane multilayer. These ratios have been expressed as $R_E(h/h')$

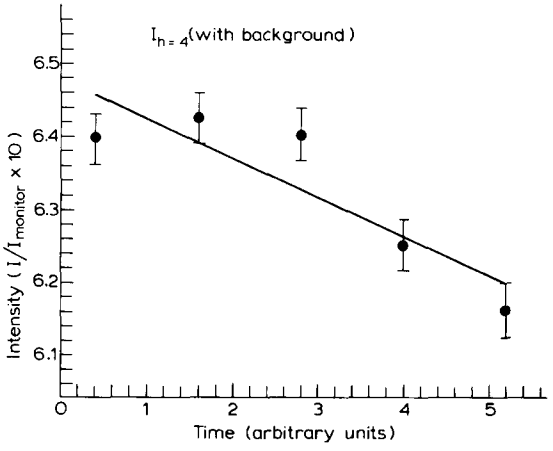

Fig. 3. The total integrated intensity including background scattering of the fourth-order reflection from a cytochrome oxidase membrane multilayer plotted as a function of time. All intensities were measured at the iron absorption edge. Error bars are computed based solely on the number of photons detected. The line represents the results of a least-squares fit to these data points. Similar plots were made for the other diffraction orders and other incident X-ray energies.

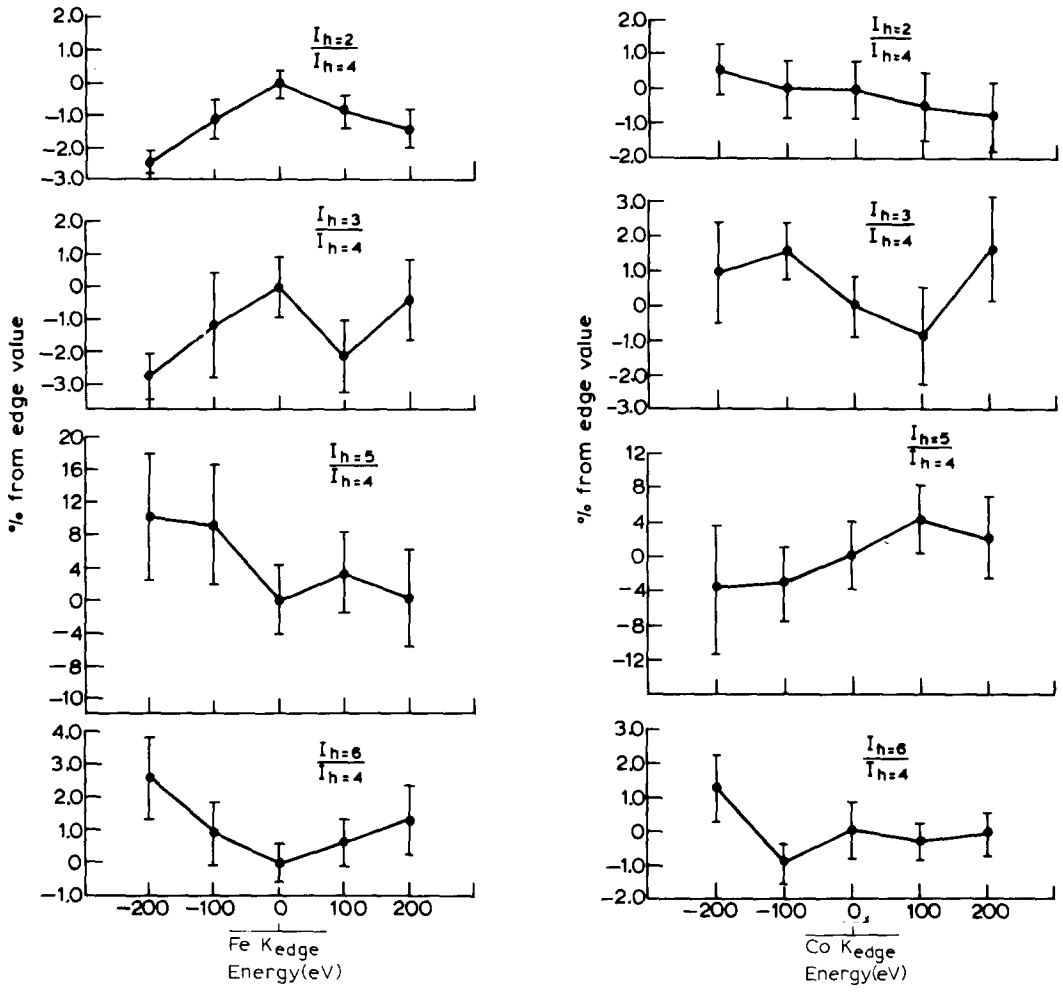

Fig. 4. (a) The ratios of the integrated intensities of the lamellar reflections, $R_E(h/h')$ (see text), for a reconstituted cytochrome oxidase membrane multilayer. $R_E(h/h')$ is shown for $h' = 4$, and $h = 2, 3, 5$ and 6 at incident X-ray energies about the iron K absorption edge. The error bars which are indicated are based on the errors in the estimated background scattering (see text). These plots show resonance diffraction effects at the iron K absorption edge. (b) The ratios $R_E(h/h')$ for $h' = 4$ and $h = 2, 3, 5$ and 6 for a reconstituted cytochrome oxidase membrane multilayer at incident X-ray energies about the cobalt K absorption edge. These plots do not show any resonance diffraction effects, which is consistent with the absence of cobalt in this membrane protein.

where:

$$R_{E2}(h/h') \equiv \frac{\left[\frac{I_{E1}(h)}{I_{E1}(h')} - \frac{I_{E2}(h)}{I_{E2}(h')}\right]}{I_{E2}(h)/I_{E2}(h')}$$

and where $E1$ denotes the incident X-ray energy of the absorption edge and $E2$ an X-ray energy far from the absorption edge. In Fig. 3a the energies are centered about the iron K edge where a resonant effect is observed for $h' = 4$ and $h = 2, 3, 5$ and 6. In this case, the average of the two values of $R_E(h/h')$ below and the two values above the K edge energy does not equal the value at the K edge energy. In Fig. 4b, the energies are centered about the cobalt K edge where no resonant effect is observed (i.e., the average value of $R_E(h/h')$ below and above the K edge equals the value at the K edge). The results are consistent with the fact that iron rather than cobalt is present in this membrane protein.

Fig. 5 shows the energy dependence of the ratios

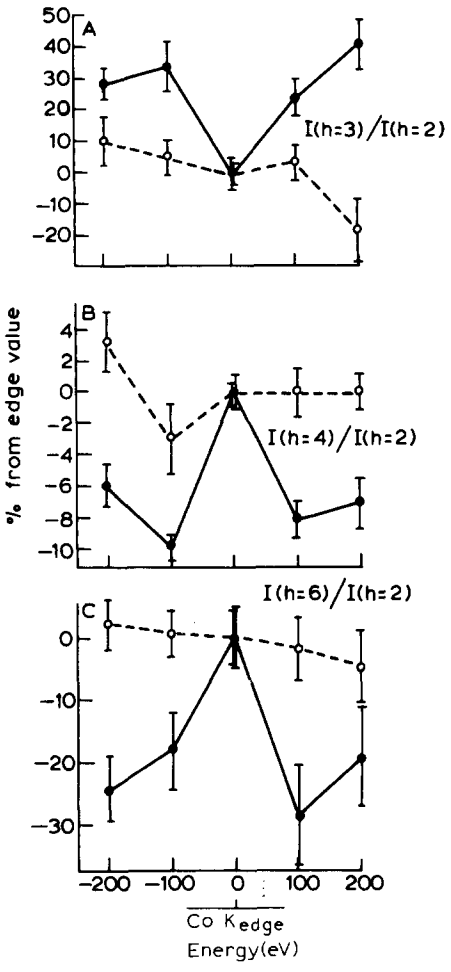

Fig. 5. The ratios $R_E(h/h')$ for $h' = 2$ and $h = 3,4$ and 6 for a reconstituted reaction center-cytochrome *c* membrane multilayer at incident X-ray energies about the cobalt K adsorption edge. The points connected by a solid line are for a sample in which the iron atom of the cytochrome *c* heme group has been replaced by cobalt. In this case, resonance diffraction effects are observed. The points connected by a dashed line are for a sample in which the iron atom of the cytochrome *c* heme group was not substituted. For this case no resonance diffraction effects were observed.

of the averaged integrated lamellar reflections, $R_E(h/h')$, for a photosynthetic reaction center-cytochrome *c* membrane multilayer. The energies are centered about the cobalt K absorption edge for $h' = 2$ and $h = 3, 4$ and 6. For points connected by a solid line, the heme iron atom of cytochrome *c* has been replaced with a cobalt atom and resonant effects are observed (i.e., the average of values above and below the K edge does not equal the value at the K edge). For points connected by a dashed line, the cytochrome *c* heme contains an iron atom and shows no resonant effects (i.e., the average of values above and below the K edge equals that at the K edge).

Discussion

Based on the total number of electrons within a single unit cell of these multilayers (10^5) and an f' K edge effect of about 8 electrons for cobalt or iron atoms, the magnitude of the resonance scattering effects should be generally approx. 0.02% of the observed intensity (Eqn. 6). Our observation of an approx. 1–20% effect demonstrates enhancement of the resonant effect due to the natural low scattering contrast of the membranes. Independent comparisons of the absolute integrated intensities of the stronger reflections with those of multilayers of dipalmitoylphosphatidylcholine (DPPC) (a lipid, the electrondensity profile of which is relatively well known on an absolute scale) shows that these membranes are of very low contrast. For example, absolute intensities corrected for the amount of material and angular disorientation show that the second-order reflection for cytochrome oxidase membranes is about 500-times weaker than the first-order reflection for DPPC. Each order is the most intense order in its respective lamellar diffraction pattern. Furthermore, background scattering between peaks indicates that the amount of incoherently scattering material is small for both cases. Therefore, absolute comparison of diffracted intensities and the known mass densities for DPPC and cytochrome oxidase membranes (which provides the same information as would the unobserved origin reflection) allows a direct comparison of electron-density profiles for the two cases. Because the structure of DPPC is known, its electron-density profile may be calculated on an absolute scale. For DPPC the difference between the maximum and average electron densities, $\Delta\rho$, is approx. 0.07 e/Å^3. Based on the comparison of the diffracted intensities and mass densities, one finds for cytochrome oxidase membranes $\Delta\rho \approx 0.01$ e/Å^3. Estimates based on this low contrast show that resonant effects exceeding 5% can be produced for the ratio of the second to fourth order diffracted intensities of this membrane multilayer. Weaker reflections would, in general, produce larger

changes (see Eqn. 6). Furthermore, generally larger resonant effects are observed for reaction center membranes which is consistent with intensity comparisons showing that these membranes have a smaller contrast, $\Delta\rho \approx 0.008$ e/Å^3, than for the cytochrome oxidase case. Therefore, the estimate of 0.02% for the magnitude of the resonant effect is the worst case and would never be realized in practice.

The observed energy dependence of $R_E(h/h')$ has a sharp fluctuation at the iron (or cobalt) edge which is roughly symmetric about the absorption edge. In this sense the energy dependence obeys an $f'(E)$ rather than an $f''(E)$ dependence for a K-shell electron. This is expected as described earlier. A more detailed examination of $f'(E)$ requires that data be collected at smaller energy intervals. The necessity to time average lamellar diffraction in order to remove sample and storage ring instabilities limited the number of different energies at which data could be recorded over a resonable amount of total time.

Finally, the resonant effect is observed at the absorption edge only when the resonant atom is known to be present in the multilayer. If the same experiment is conducted over a different energy range where no resonances exist, the effect is not observed. On the other hand, the resonant effect over a fixed energy range may appear or vanish by chemically adding or removing the resonant atom.

The use of ratios of integrated intensities approximately eliminates nonresonant and absorption energy dependencies. If h is the order of the reflection and E is the energy, then in general:

$$I(h, E) \cong |F(h)|^2 T(E, h) \tag{10}$$

where $T(E, h)$ is the experimental transfer function containing nonresonant and absorption terms. From Eqn. 10, it is clear that the ratio of intensities removes nonresonant energy dependencies if E and h are uncoupled in T. However, from Eqn. 8, although the ratio now depends only on the resonant scattering effect, the magnitude of the signal is determined by the unit cell's contrast as well as the location of the resonant atom in the unit cell profile. If $T(E, h)$ were independently known, then the quantity:

$$\frac{I(h, E \ll E_K) - I(h, E \approx E_K)}{I(h', E \ll E_K) - I(h', E \approx E_K)} \tag{11}$$

would depend only on the resonant atom's position in the unit cell. Thus, future experiments which permit independent calibration of the function $T(E, h)$ would significantly enhance the method's ability to locate resonant atoms.

Therefore, based on the magnitude and energy dependence of the $R_E(h/h')$ and the control experiments performed, these data suggest that the resonance diffraction effect has indeed been observed in the lamellar diffraction from these reconstituted membrane multilayers. These and further experiments which measure such effects more accurately can be used to determine the location of these resonant atoms (and therefore the active sites with which they are associated) in the membrane profile [9]. Errors in this experiment remain at the 0.5% level. Further reduction in errors should be possible with advanced linear or area X-ray detectors which will better define the background scattering and shorten the data collection time (reducing the effects of sample and storage ring instabilities).

References

1 Stamatoff, J., Bilash, T., Ching, Y. and Eisenberger, P. (1979) Biophys. J. 28, 413–421

2 Blasie, J.K., Schoenborn B.P. and Zaccai, G. (1976) Direct Methods for the Analysis of Lamellar Neutron Diffraction from Oriented Multilayers: A Difference Patterson Deconvolution Approach, Brookhaven Symposium in Biology No. 27, Neutron Scattering for the Analysis of Biological Structures

3 King, G.I., Mowery, P.C., Stoeckenius, W., Crespi, H.L. and Schoenborn, B.P. (1980) Proc. Natl Acad. Sci. U.S.A. 77, 4726–4730

4 Stamatoff, J., Powers, L., Eisenberger, P., Wickman, H.H. and Lytz, R.K. (1978) Biophys. J. 21, 204a

5 Baldeschwieler, J.D., Chan, S.I., Gamble, R.C. and Trentacosti, F.L. (1978) Anomalous Scattering and Fine Structure in the Scattering Factor Curve, Stanford Synchrotron Radiation Laboratory Activity Report 78/10, Stanford Synchroton Radiation Laboratory.

6 Stuhrmann, H.B. (1981) Acta Crystallogr. A, in the press.

7 Lye, R.C., Phillips, J.C., Kaplan, D., Doniach, S. and Hodgson, K.O. (1980) Proc. Natl. Acad. Sci. U.S.A. 77, 5884–5888

8 Fuoss, P.H., Eisenberger, P., Warburton, W.K. and Bienenstock, A. (1981) Phys. Rev. Lett, in the press

9 Blasie, J.K., Pachence, J.M., Tavormina, A., Erecinska, M., Dutton, P.L., Stamatoff, J., Eisenberger P. and Brown, G. (1982) Biochim. Biophys. Acta 679, 188–197

10 Hönl, H. (1933) Z. Phys. 84, 1–16

11 James, R.W. (1948) in The Crystalline State (Bragg, L., ed.), vol. 2, Cornell University Press, Ithaca
12 Kawamura, T. and Fukamachi, T. (1978) Jap. Appl. Phys. 17, 224–226
13 Pachence, J.M., Dutton, P.L. and Blasie, J.K. (1979) Biochim. Biophys. Acta 548, 348–373
14 Eytan, G.D. and Broza, R. (1978) J. Biol. Chem. 253, 3196–3202
15 Vanderkoi, J.M., Adar, F. and Erecinska, M. (1976) Eur. J. Biochem. 64, 381–387